

VU Research Portal

Loss of Rb proteins: Consequences for cell cycle control and genome integrity

van Harn, T.

2013

document version

Publisher's PDF, also known as Version of record

[Link to publication in VU Research Portal](#)

citation for published version (APA)

van Harn, T. (2013). *Loss of Rb proteins: Consequences for cell cycle control and genome integrity*. [PhD-Thesis – Research external, graduation internal, Vrije Universiteit Amsterdam].

General rights

Copyright and moral rights for the publications made accessible in the public portal are retained by the authors and/or other copyright owners and it is a condition of accessing publications that users recognise and abide by the legal requirements associated with these rights.

- Users may download and print one copy of any publication from the public portal for the purpose of private study or research.
- You may not further distribute the material or use it for any profit-making activity or commercial gain
- You may freely distribute the URL identifying the publication in the public portal ?

Take down policy

If you believe that this document breaches copyright please contact us providing details, and we will remove access to the work immediately and investigate your claim.

E-mail address:

vuresearchportal.ub@vu.nl

Chapter 2

LOSS OF RB PROTEINS CAUSES GENOMIC INSTABILITY IN THE ABSENCE OF MITOGENIC SIGNALING

Tanja van Harn^{*,1}

Floris Foijer^{*,1,2}

Marcel van Vugt³

Ruby Banerjee²

Fentang Yang²

Anneke Oostra⁴

Hans Joenje⁴

Hein te Riele¹

Genes and Development
2010 Jul 1;24(13):1377-88

*: These authors contributed equally

¹: Division of Molecular Biology; The Netherlands Cancer Institute; Amsterdam; The Netherlands

²: Wellcome Trust Genome Campus; Wellcome Trust Sanger Institute; Cambridge; UK

³: Department of Medical Oncology; Groningen Medical Centre; Groningen; The Netherlands

⁴: Department of Clinical Genetics; VU University Medical Center; Amsterdam; The Netherlands

2

Abstract

Loss of G1/S control is a hallmark of cancer and is often caused by inactivation of the retinoblastoma pathway. However, Mouse Embryonic Fibroblasts lacking the retinoblastoma genes *RB1*, *p107* and *p130* (TKO MEFs) are still subject to cell cycle control: upon mitogen deprivation they enter and complete S phase, but then firmly arrest in G2. We now show that G2-arrested TKO MEFs have accumulated DNA damage. Upon mitogen re-addition, cells resume proliferation, although only part of the damage is repaired. As a result, mitotic cells show chromatid breaks and chromatid cohesion defects. These aberrations lead to aneuploidy in the descendent cell population. Thus, our results demonstrate that unfavorable growth conditions can cause genomic instability in cells lacking G1/S control. This mechanism may allow pre-malignant tumor cells to acquire additional genetic alterations that promote tumorigenesis.

Introduction

Cancer cells have successively acquired multiple genetic and/or epigenetic alterations that permit unrestrained proliferation. The G1 checkpoint, which is an important barrier to proliferation under growth inhibitory conditions, is frequently mutated in human tumors by various perturbations in the retinoblastoma (Rb) tumor suppressor pathway (Malumbres and Barbacid 2001). Loss of function of the *RB1* gene is the initiator event in retinoblastoma, a pediatric cancer of the eye (Corson and Gallie 2007; Dimaras et al. 2008). Additionally, inactivation of *RB1* was found in various other tumors like sporadic breast, bladder, prostate and small cell lung carcinoma. Abrogation of the G1 checkpoint can also occur by genetic alteration of upstream regulators of the Rb pathway. Amplification of *Cyclin D1* was found in breast, esophagus and head and neck cancer and loss of p16^{INK4A} function was observed in melanoma and pancreatic and bladder carcinomas (Malumbres and Barbacid 2001). Moreover, human papillomavirus (HPV) can initiate cervical carcinoma and squamous cell carcinoma of the head and neck by expression of the E7 oncoprotein that inactivates pRB (Doorbar 2006; Perez-Ordóñez et al. 2006).

Besides loss of cell cycle control mechanisms, genomic instability manifested by aneuploidy and chromosomal rearrangements, is another hallmark of solid tumors (Marx 2002) and has also been observed in retinoblastomas (Dimaras et al. 2008). Genomic instability may be due to defects in genome maintenance mechanisms by loss, mutation or epigenetic silencing of genes encoding DNA repair enzymes and checkpoint proteins (Harper and Elledge 2007). However, it has also been suggested that interference with pRB function could promote polyploidy, aberrations in chromosome number or micronuclei formation (Zheng et al. 2002; Hernando et al. 2004; Gonzalo et al. 2005; Mayhew et al. 2005; Iovino et al. 2006; Srinivasan et al. 2007; Amato et al. 2009). How these alterations originate in pRB depleted cells is not entirely understood. It has been suggested that DNA Double Strand Breaks (DSBs) are not properly repaired in pRB depleted cells. S-phase cells exposed to genotoxic stress slow down replication fork progression to suppress the formation of DSBs (Bosco et al. 2004). This process required dephosphorylation of pRB (Knudsen et al. 2000) and therefore the inability of pRB-defective cells to decelerate S-phase progression could promote DNA damage. Furthermore, pRB deficiency was also shown to attenuate the DNA-damage-induced G2 checkpoint due to the up-regulation of many genes required for G2/M progression (Hernando et al. 2004; Jackson et al. 2005; Eguchi et al. 2007). These imperfections in S and G2 checkpoints in pRB-defective cells may impede efficient DNA damage repair and cause aberrant chromosome segregation during mitosis. As a result various other genes that could promote tumorigenesis may become abnormally expressed. Thus, loss of pRB function that abrogates the G1 checkpoint may also induce genomic instability and accelerate tumor development.

In cultured cells, depletion of mitogens results in G1 arrest. This arrest is established by inhibition of Cyclin-CDK activity (Cyclin D–CDK4/6 complexes) resulting in hypophosphorylation of the retinoblastoma (Rb) proteins, which besides pRB compromise p107 and p130. Hypophosphorylated Rb proteins can sequester E2F transcription factors and by recruiting chromatin modifiers like HDACs, DNMT1, HP1A and Suv39H1 inhibit the transcription of E2F target genes required for S phase progression (Burkhardt and Sage 2008). The G1 arrest critically depends on the Rb proteins since complete disruption of the genes encoding pRB, p130 and p107 in Mouse Embryonic Fibroblasts (hereafter referred to as TKO MEFs) abrogated the capacity of these cells to arrest in the G1 phase of the cell cycle (Dannenberg et al. 2000; Sage et al. 2000).

However, TKO MEFs were not refractory to mitogen deprivation. Although Rb proteins contribute to the G2 arrest in response to DNA damage (Jackson et al. 2005; Eguchi et al. 2007), we have found that mitogen deprivation of TKO MEFs in which the apoptotic response was suppressed by over-expression of the anti-apoptotic protein Bcl2 caused a robust G2 arrest (Fojier et al. 2005). This cell cycle block was accomplished by up-regulation of the cyclin-dependent kinase inhibitors (CKIs) p27^{Kip1} and p21^{Cip1} that were found to bind to and inactivate the Cyclin-CDK complexes that are required for G2/M progression.

The accumulation of p27^{Kip1} most likely resulted from down-regulation of PI-3 kinase activity upon mitogen deprivation (Fojier et al. 2008) that activates the Forkhead transcription factors stimulating the transcription of p27^{Kip1} (Medema et al. 2000). However, we also observed up-regulation of p21^{Cip1}. Since p21^{Cip1} accumulation in mitogen-starved TKO MEFs was shown to be dependent on ATM/ATR kinase activity and the presence of p53 (Fojier et al. 2005), we wondered whether the up-regulation of p21^{Cip1} was due to the presence of DNA damage. In the present study we show that mitogen-starved, G2-arrested TKO-Bcl2 MEFs had accumulated many DSBs, which upon re-stimulation of cells by mitogen addition were not completely repaired. In addition, chromosomes showed severe loss of centromeric cohesion. These phenomena may be responsible for copy number alterations that were frequently found in descendent cell clones.

Results

The DNA Damage Response delays cell cycle re-entry of G2 arrested TKO-Bcl2 MEFs

TKO-Bcl2 MEFs that had arrested in G2 by 7 days of mitogen deprivation (Figure 1A, right panel) had accumulated high levels of the CKIs p27^{Kip1} and p21^{Cip1} (Fojier et al. 2005). These cells were able to re-enter the cell cycle by re-addition of 10% FCS, but interestingly, serum re-addition did not result in decreased p21^{Cip1} protein levels (Fojier et al. 2005) and caused an up-regulation of DNA damage response genes (Fojier et al. 2008). We therefore speculated that serum-starved TKO-Bcl2 MEFs have accumulated DNA damage. Such damage would activate the DNA Damage Response (DDR), which results in the recruitment of ATM and phosphorylation of the histone variant H2AX (γ -H2AX) (Harper and Elledge 2007). To obtain evidence for activation of the DDR, we studied the rate of cell cycle re-entry upon serum re-addition in the presence of either caffeine, an inhibitor of the ATM/ATR kinases (Sarkaria et al. 1999) or UCN-01, an inhibitor of the downstream kinase CHK1 (Graves et al. 2000). Figures 1B and 1C show that upon serum re-addition the appearance of mitotic cells was accelerated by caffeine; the appearance of mitotic TKO-Bcl2 MEFs after stimulation with only 10% FCS peaked 6 hours later than after stimulation with 10% FCS in the presence of caffeine. Also UCN-01 accelerated mitotic entry of serum re-stimulated TKO-Bcl2 MEFs (Figure S1). Furthermore, we found that re-stimulation in the absence of caffeine led to a rapid down-regulation of p27^{Kip1}, but not p21^{Cip1} levels (Fig. 1D, lane 2-6). However, in the presence of caffeine, also p21^{Cip1} levels rapidly declined (Figure 1D; compare lane 7-11 with lane 2-6). These results demonstrate that cell cycle re-entry of serum-starved TKO-Bcl2 MEFs was hampered by the DDR, which is indicative for the presence of DNA damage. We also noticed that treatment with caffeine accelerated cell cycle re-entry, but did apparently not result in progression to G1 phase as after 24 hours only few cells with a 2n DNA content were present, in contrast to re-stimulation with 10% serum only (Figure 1B, 24h panels). This may indicate that in the presence of caffeine, cells entered mitosis with a high amount of DNA damage that impeded proper mitosis and/or cytokinesis.

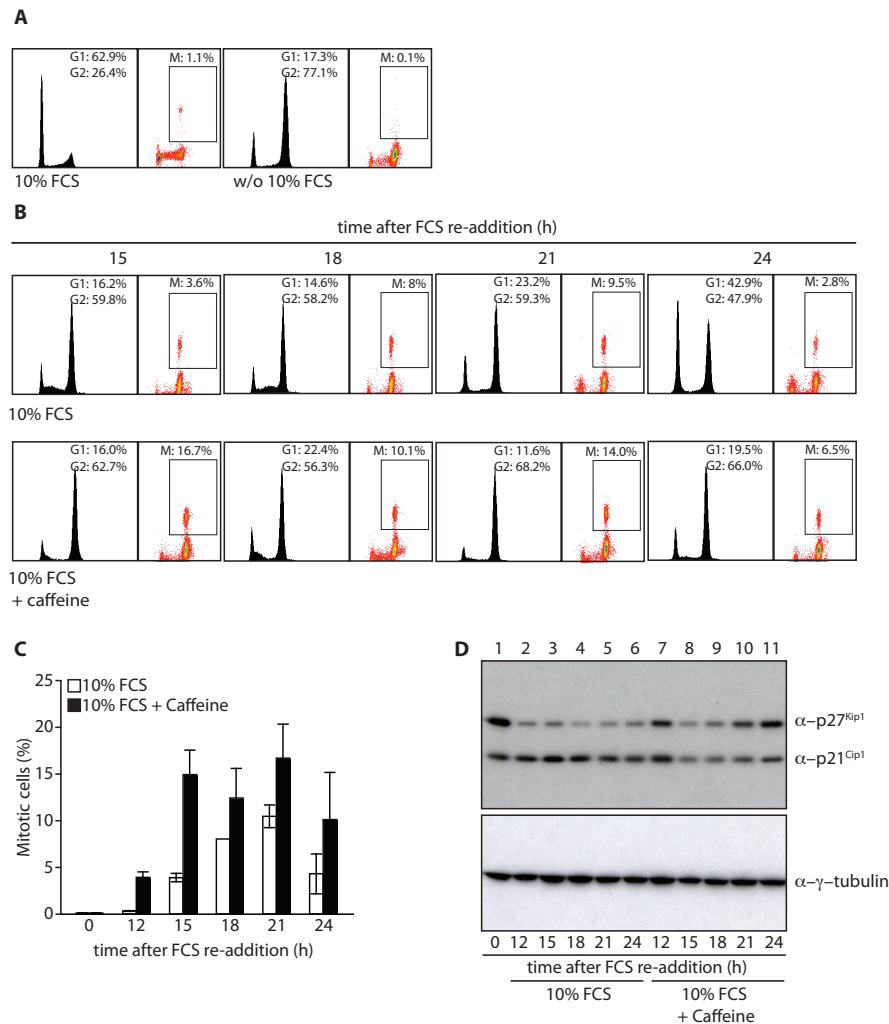


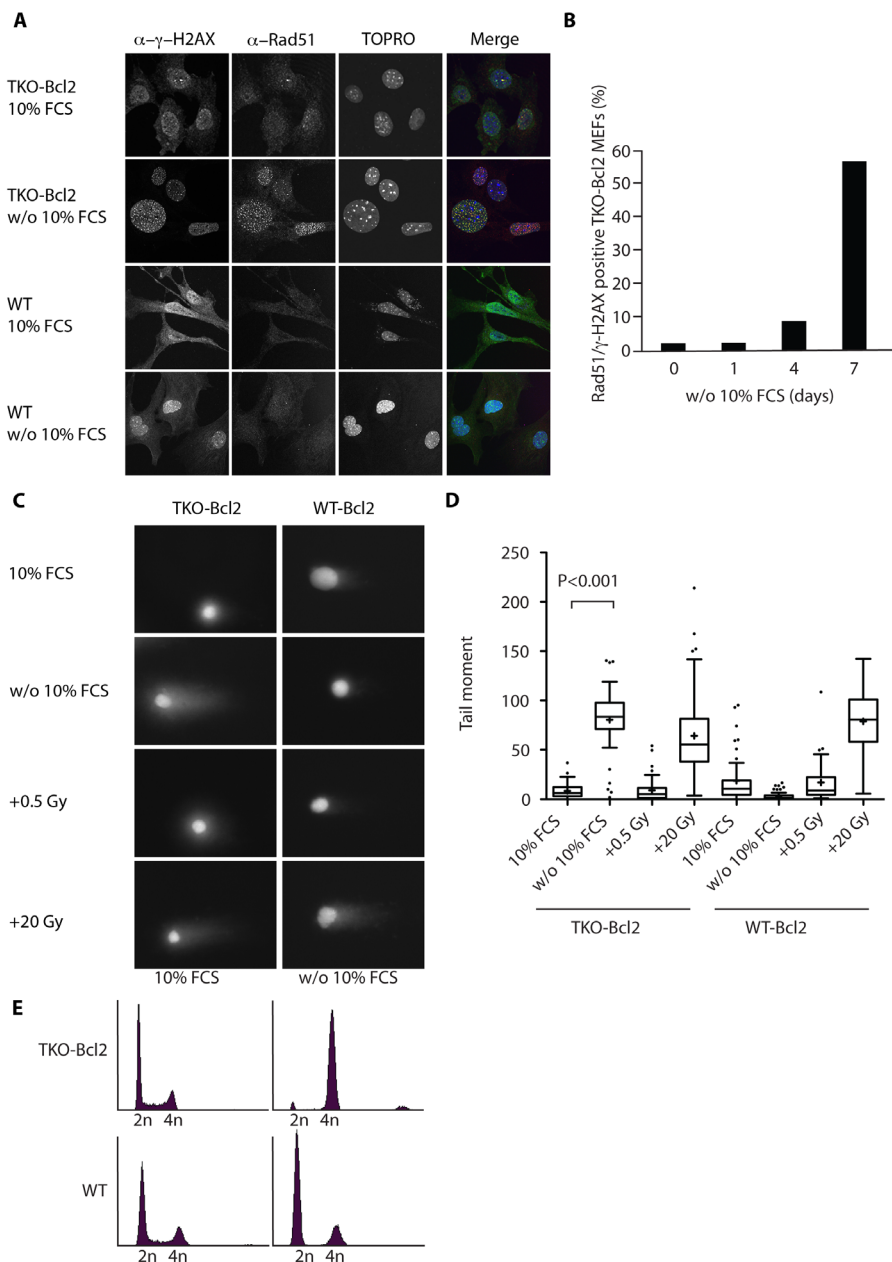
Figure 1: Inhibition of the DDR results in accelerated cell cycle re-entry of G2-arrested TKO-Bcl2 MEFs after serum re-addition

(A) Cell cycle distribution and percentage of mitotic cells as measured by MPM2 positivity in TKO-Bcl2 MEFs cultured in the presence or absence (w/o) of 10% FCS (for 7 days) (B) and in serum-starved TKO-Bcl2 MEF cultures re-stimulated with 10% FCS for 15, 18, 21 and 24 h in the presence (lower part) or absence of caffeine (upper part). (C) Percentage of mitotic cells in TKO-Bcl2 MEFs at different time points after serum re-addition either in the presence (black bars) or absence (white bars) of caffeine. Graph represents average values of two independent experiments, error bars show standard deviations. (D) p27^{Kip1} and p21^{Cip1} protein levels in TKO-Bcl2 MEFs at different time points after serum re-addition either in the presence (lane 7-11) or absence (lane 2-6) of caffeine. Anti γ -tubulin was used as loading control.

DNA damage in mitogen-deprived TKO-Bcl2 MEFs

Nuclear foci that are positive for both γ -H2AX and Rad51, a protein involved in homologous recombination by promoting strand invasion (Branzei and Foiani 2008), are indicative for the presence of DSBs (Paull et al. 2000). Figure 2A shows that such foci were present in mitogen-deprived TKO-Bcl2 MEFs, but absent in TKO-Bcl2 MEFs cultured in the presence of

10% FCS as well as in wildtype (WT) MEFs cultured in the presence or absence of 10% FCS. The percentage of TKO-Bcl2 MEFs carrying more than five γ -H2AX/Rad51 foci gradually increased upon serum deprivation to reach 60% after 7 days of mitogen deprivation (Figure 2B).



< Figure 2: Serum deprived TKO-Bcl2 MEFs contain DSBs

(A) Immunofluorescent images of TKO-Bcl2 and WT MEFs cultured in the presence or absence of 10% FCS (for 7 days) to detect γ -H2AX and Rad51 foci. DNA was labeled with TOPRO-3. In the merge picture DNA is blue, γ -H2AX is green, Rad51 is red and colocalization of γ -H2AX and Rad51 is seen as yellow foci. (B) Quantification of γ -H2AX/Rad51 focus formation in TKO-Bcl2 MEFs cultured without 10% FCS for 1, 4 and 7 days. Cells were considered positive when they contained five or more superimposed γ -H2AX and Rad51 foci. At least 100 cells were counted for each condition. (C) Representative comets of nuclei of TKO-Bcl2 and WT-Bcl2 MEFs stained with Propidium Iodide cultured in the presence or absence of 10% FCS (for 7 days). Cells exposed to 0.5 or 20 Gy of γ -irradiation served as controls. (D) Tail moments obtained from TKO-Bcl2 and WT-Bcl2 MEFs cultured in the presence (untreated or γ -irradiated with 0.5 or 20 Gy) or absence of 10% FCS (for 7 days). Box plots represent interquartile ranges, horizontal bars denote the median, plus (+) indicates the mean value and points indicate outliers. For each condition 50 cells were analyzed using the CASP software. (E) Cell cycle distribution as determined by Propidium Iodide staining of TKO-Bcl2 and WT MEFs cultured in the presence or absence of 10% FCS (for 7 days).

We also assessed the presence of γ -H2AX/Rad51 foci in cells lacking pRB and p107 since these cells only partially arrested in G2 upon mitogen withdrawal (Fojier et al. 2005) (Figure S2A) and loss of these two Rb proteins strongly stimulated development of retinoblastoma and other tumors in mice (Dannenberg et al. 2004). In mitogen-starved *Rb*^{-/-}*p107*^{-/-} MEFs both p27^{Kip1} and p21^{Cip1} protein levels were up-regulated (Figure S2B) and the number of cells positive for γ -H2AX/Rad51 foci corresponded to the number of cells arrested in G2 (Figure S2C and S2D).

Rad51 is expressed during late G1, S and G2 phase of the cell cycle in murine cells (Yamamoto et al. 1996) and might therefore be a poor indicator of DSBs in early G1. To confirm the presence of DSBs in G2-arrested TKO-Bcl2 MEFs and their absence in G1-arrested WT MEFs (Figure 2E), we assessed the presence of DSBs by performing neutral comet assays (Olive and Banath 2006). Comets could readily be detected in mitogen-deprived TKO-Bcl2 MEFs while they were absent in TKO-Bcl2 MEFs cultured in the presence of 10% FCS and in WT-Bcl2 MEFs cultured in the presence or absence of 10% FCS (Figure 2C). Figure 2D shows that the mean tail moment, a quantitative indicator for the presence of DSBs, was significantly increased in mitogen-deprived TKO-Bcl2 MEFs, but not in mitogen-deprived WT-Bcl2 MEFs. In contrast, when TKO-Bcl2 MEFs and WT-Bcl2 MEFs were exposed to ionizing radiation (20 Gy), both cell types showed comets with comparable tail moments (Figures 2C and D).

Thus, lack of pocket protein activity in combination with mitogen deprivation resulted in the formation of DSBs. Since WT MEFs did not contain DSBs and arrested in the G1 phase of the cell cycle upon mitogen withdrawal (Figure 2E), these results indicate that the progression through an unscheduled S-phase might be the cause of DSB formation.

Serum re-stimulated TKO-Bcl2 MEFs re-entered the cell cycle with DNA damage

To examine whether cell cycle re-entry upon serum re-addition was accompanied by DNA repair, we quantified the percentage of TKO-Bcl2 MEFs containing more than five γ -H2AX/Rad51 foci during incubation following serum re-addition (Figure 3B). 21 hours after serum re-addition the number of cells containing γ -H2AX/Rad51 foci had decreased more than twofold, suggesting that repair had occurred. However, at 15 hours, the number of cells carrying more than five foci had not yet decreased while at this time the first cells had started to enter mitosis (Figure 3A).

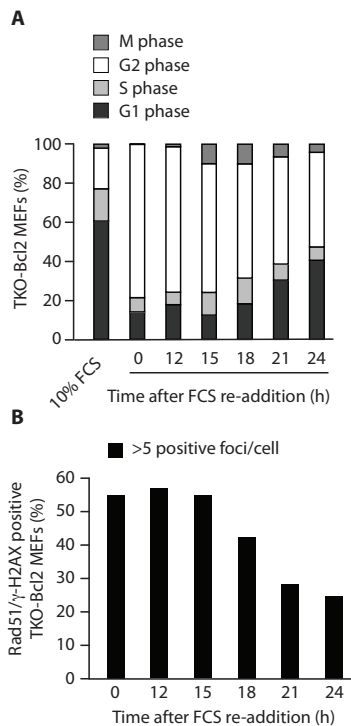


Figure 3: γ -H2AX/Rad51 foci partially dissolve when serum re-stimulated TKO-Bcl2 MEFs re-enter the cell cycle

(A) Cell cycle distribution and percentage of mitotic cells in TKO-Bcl2 MEF cultures at different time points after FCS re-addition. The percentages depicted in this graph represent 5 independent experiments. (B) Quantification of γ -H2AX/Rad51 foci in TKO-Bcl2 MEFs after FCS re-addition. Cells were considered positive when they contained five or more foci positive for both γ -H2AX and Rad51. At least 100 cells were counted for each condition.

Since it has previously been shown that Rb deficiency resulted in a less stringent G2 arrest in response to DNA damaging agents (Jackson et al. 2005; Eguchi et al. 2007), it could be possible that serum re-stimulated TKO-Bcl2 MEFs re-entered the cell cycle with unrepaired DSBs. This was already suggested by the persistent elevated levels of p21^{Cip1} in serum re-stimulated TKO-Bcl2 MEFs (Figure 1C, lanes 1-6) that were progressing into mitosis (Figure 3A). To examine this further, we followed serum re-stimulated TKO-Bcl2 MEFs by time-lapse microscopy. As a readout for DSBs, we monitored the presence of foci containing 53BP1, a mediator protein recruited to DSBs (Schultz et al. 2000). To this aim, a fusion protein of 53BP1 and GFP was expressed in TKO-Bcl2 MEFs. Expression of 53BP1-GFP did not interfere with mitotic entry of G2-arrested TKO-Bcl2 MEFs after serum re-addition (Figure S3), nor did it result in the formation of aggregates in cycling cells that could be misinterpreted as DNA damage foci (Figure 4B). Figure 4A shows two mitogen-deprived TKO-Bcl2 MEFs that still contained numerous 53BP1-GFP foci at 21 hours after serum re-addition (marked with + and ^). Eventually, these cells progressed into mitosis (27.5 and 31.5 hours after serum re-addition, respectively) with a clear decrease in the number of 53BP1-GFP foci. Nevertheless, one daughter cell still harbored some 53BP1-GFP foci after cytokinesis (marked with +, 36 hours after FCS re-addition; upper cell). This indicates that not all the DSBs in this cell were completely repaired before mitotic entry. Fifty-eight percent (30/52) of the TKO-Bcl2 + 53BP1-GFP MEFs we were able to follow for several hours before mitotic entry contained 53BP1-GFP foci. Strikingly, fifty-three percent (25/47) of the cells we could examine after cellular division still had 53BP1-GFP foci, although the number of foci was clearly reduced as illustrated in Figure 4A (and data not shown). Thus, serum-restimulated TKO-Bcl2 MEFs re-entered the cell cycle in the presence of DNA damage foci indicative for remaining DSBs.

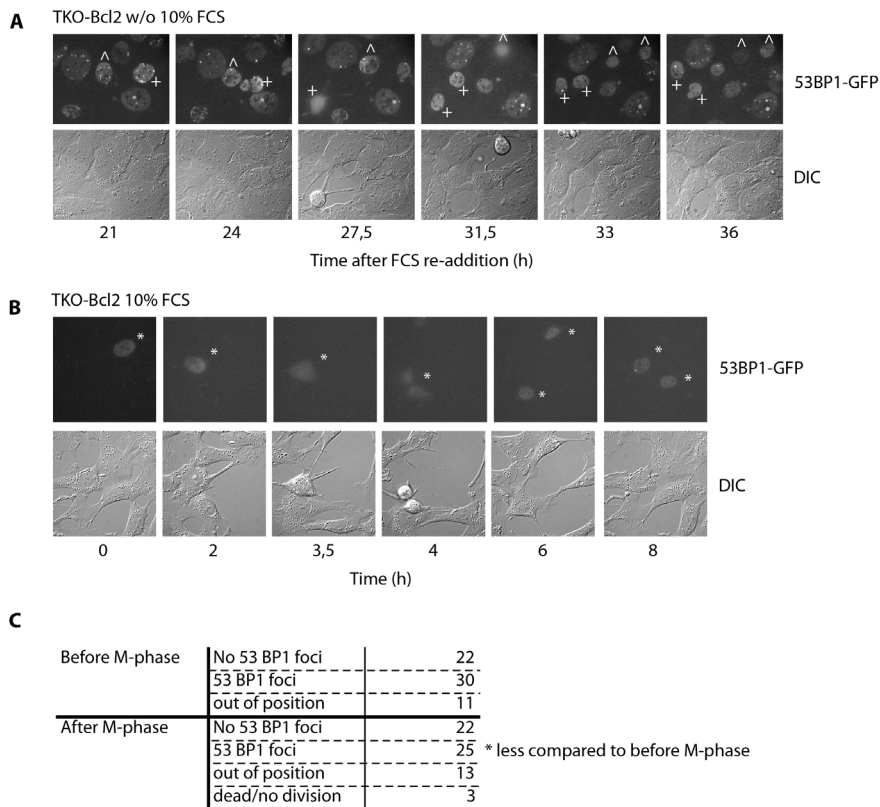


Figure 4: Live cell imaging of TKO-Bcl2 MEFs expressing 53BP1-GFP

(A) 53BP1-GFP foci in mitogen-deprived TKO-Bcl2 MEFs re-stimulated with serum for the indicated times. TKO-Bcl2 MEFs that entered mitosis are marked with ^ and +. (B) 53BP1-GFP positive TKO-Bcl2 MEF (marked with *) going through mitosis cultured in the presence of 10% FCS continuously. (C) Quantification of the number of serum re-stimulated TKO-Bcl2 MEFs containing 53BP1-GFP foci before and after M-phase.

Chromosome abnormalities

To examine the presence of DNA damage in mitogen-deprived TKO-Bcl2 MEFs that had re-entered the cell cycle after serum re-addition, we screened for chromosomal abnormalities in metaphase spreads from cells that were harvested 21 hours after serum re-addition. TKO-Bcl2 MEFs and WT MEFs hardly contained break events when they had always been cultured in the presence of 10% FCS (Figure 5A). In contrast, in serum deprived TKO-Bcl2 MEFs that were restimulated to enter mitosis, numerous chromatid breaks were present (Figures 5B and 5F; indicated by arrows). Chromatid breaks were hardly observed in serum-starved and re-stimulated WT MEFs (Figures 5B and 5E), once more suggesting that progression through an aberrant S-phase in the absence of mitogens resulted in chromosomal abnormalities.

In addition to chromatid breakages, we also observed defects in centromeric sister chromatid cohesion, as evidenced by a railroad-track appearance of chromosomes (Figure 5F; indicated by arrowheads). Figure 5D illustrates that in 90% of serum re-stimulated TKO-Bcl2 MEFs more than 10 metaphase chromosomes no longer showed the typical tight centromeric cohesion. This sharply contrasts to serum re-stimulated WT MEFs (Figures 5D and E) as well as TKO-Bcl2 and WT MEFs cultured in the presence of 10% FCS continuously (Figure 5C) wherein the

majority of cells did not show signs of loss of centromeric sister chromatid cohesion.

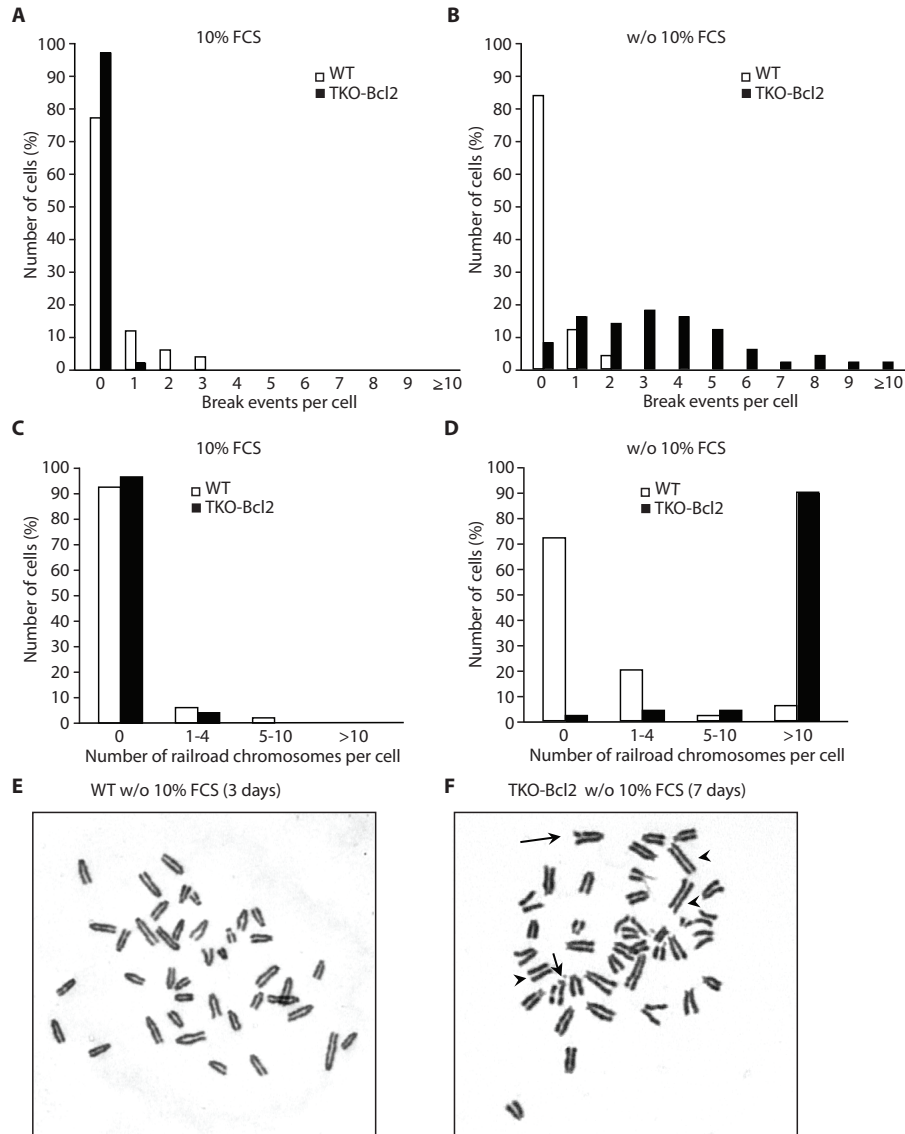


Figure 5: Serum deprivation of TKO-Bcl2 MEFs results in chromosomal aberrations

(A-B) Quantification of chromosomal breakage events in (A) proliferating TKO-Bcl2 MEFs and WT MEFs, (B) serum re-stimulated (21 hours) TKO-Bcl2 MEFs after 7 days of mitogen deprivation and serum re-stimulated WT MEFs after 3 days of mitogen deprivation. (C-D) Quantification of loss of centromeric cohesion in (C) proliferating TKO-Bcl2 MEFs and WT MEFs, (D) serum re-stimulated (21 hours) TKO-Bcl2 MEFs after 7 days of mitogen deprivation and serum re-stimulated WT MEFs after 3 days of mitogen deprivation. (a-d) Per condition 50 metaphases were evaluated. (E,F) Chromosome spread of (E) serum re-stimulated WT MEFs after 3 days of mitogen deprivation. (F) serum re-stimulated (21 hours) TKO-Bcl2 MEFs after 7 days of mitogen deprivation. Arrows indicate chromatid breaks; arrowheads indicate railroad chromosomes.

Sister chromatid cohesion is established during S-phase by the cohesin complex (Peters et al. 2008). We determined whether inappropriate entry into S-phase under growth-restricting conditions resulted in defects in cohesin loading. Figure S4A shows that the levels of chromatin-associated Rad21, a subunit of the cohesin complex, did not differ between cells cultured in the presence or absence of 10% FCS, suggesting that the loading was not defective. This corresponds to the work of Manning et al. showing that compromised sister chromatid cohesion in pRB depleted cells was not caused by loss of chromatin-associated cohesin complexes. Apart from loading defects, it is possible that the cohesin complex was removed prematurely during mitogen re-addition. To exclude this, we assessed whether cohesion defects were already present in G2 arrested TKO-Bcl2 MEFs before serum-restimulation. To this aim, G2 arrested cells were treated with Calyculin A that induces premature chromosome condensation and thus allows the visualization of chromosomes in G2 (Gotoh 2009). Similar to metaphase spreads from re-stimulated TKO-Bcl2 MEFs, chromosome spreads from G2 arrested cells showed chromosome breaks and loss of centromeric cohesion (Figure S4B). Thus, although the cohesin complex was loaded properly onto the chromatin, the defects in sister chromatid cohesion were already present in G2 arrested cells, suggesting they had occurred in the preceeding S phase.

	CGH	M-FISH	
		Most spreads	Some spreads
1 (10%FCS)	No changes		Loss chr. 6 Transl. (6;6) Transl. (2;6)
2 (10% FCS)	No changes		Loss chr. 11, 14 Gain chr. 17
3 (10% FCS)	No changes		Gain chr. 3, 5, 8, Y Loss chr. 12, 14
4 (10% FCS)	No changes	n.d.	n.d.
5 (10% FCS)	No changes	n.d.	n.d.
6 (10% FCS)	No changes	n.d.	n.d.
7 (10% FCS)	No changes	n.d.	n.d.
8 (10% FCS)	No changes	n.d.	n.d.
9 (10% FCS)	Loss chr. 1 (part) Gain chr. 8, 11	n.d.	n.d.
10 (10% FCS)	No changes	n.d.	n.d.
11 (10% FCS)	Gain chr. 10 (part)	n.d.	n.d.
1 (w/o 10% FCS)	No changes		Gain chr. 6, 7, 8, 12, 15 Loss chr. 14
2 (w/o 10% FCS)	No changes		Loss chr. 12, Y
3 (w/o 10% FCS)	No changes		Gain chr. 7, 8, 12, Y Loss chr. Y Gain chr. 4
4 (w/o 10% FCS)	No changes		Transl. (8;11) Loss chr. 3
5 (w/o 10% FCS)	Loss chr. 12 (part) Gain chr. 15	Transl. (12;15)	
6 (w/o 10% FCS)	Loss chr. 7	Loss chr. Y	Loss chr. 4, 19 Gain chr. 5, 17
7 (w/o 10% FCS)	Loss chr. 8, 11	Loss chr. 7, 8, 11	Loss chr. 1, 9, 12, 13, 14, 16, 18, Y Gain chr. 2, 6, 7, 13, 15, 16, 19 Transl. (6;7), (8;17)
8 (w/o 10% FCS)	Loss chr. 1, 7, 12 Mini chr. 5	Loss chr. 1, 7, 8, 12, 14	Loss chr. 3, 11, 13, 17, Y Gain chr. 2, 4, 6, 9, 10, 11, 13, 15, 17, 19, Y
9 (w/o 10% FCS)	Loss chr. 14, 17	n.d.	n.d.
10 (w/o 10% FCS)	No changes	n.d.	n.d.
11 (w/o 10% FCS)	No changes	n.d.	n.d.
12 (w/o 10% FCS)	No changes	n.d.	n.d.
13 (w/o 10% FCS)	Loss chr. 14	n.d.	n.d.

Table 1: Summary of the numerical and structural aberrations detected by CGH and M-FISH in single cell clones derived from TKO-Bcl2 MEFs cultured in the presence or absence of 10% FCS

Most spreads: more than 50% of the metaphase spreads, some spreads: less than 50% of the metaphase spreads (Chr.: chromosome; Transl.: translocation; n.d.: not determined).

Genomic instability

We have previously observed that proliferating cell cultures could be obtained from serum re-stimulated TKO-Bcl2 MEFs (Foijer et al. 2005). To investigate whether the numerous chromatid breaks and losses of centromeric cohesion in serum-stimulated TKO-Bcl2 MEFs gave rise to numerical or structural chromosomal alterations in this proliferating population, we generated 13 clones from single cells. These clones were analyzed by array-based Comparative Genomic Hybridization (aCGH) for copy number alterations (CNAs). Eight of the 13 clones were obtained from single cells that were in mitosis 21 hours after serum re-addition (Table 1, clone 6-13 w/o 10% FCS). In five of these clones, we detected CNAs. Since these re-stimulated cells had entered M-phase relatively late (Figure 1B) and may thus be more severely damaged, we might have over-estimated the presence of chromosomal aberrations in the entire proliferating population. Therefore, we also analyzed five clones generated from single cells out of the whole cell population obtained 48 hours after serum re-addition (Table 1, clone 1-5 w/o 10% FCS). In this case, severely damaged cells may have been counter-selected as non- or moderately-damaged cells may have entered the cell cycle earlier and dominated the population. Nevertheless, also in this case we observed chromosome aberrations in one clone that had gained chromosome 15 and lost part of chromosome 12 (Figure 6A). Thus, in 46% of all clones derived from serum-starved TKO-Bcl2 MEFs, we found CNAs. In contrast, we detected CNAs in only 16% of cell clones derived from TKO-Bcl2 MEFs that had always been cultured in the presence of 10% FCS (Table 1, clone 1-11 10% FCS).

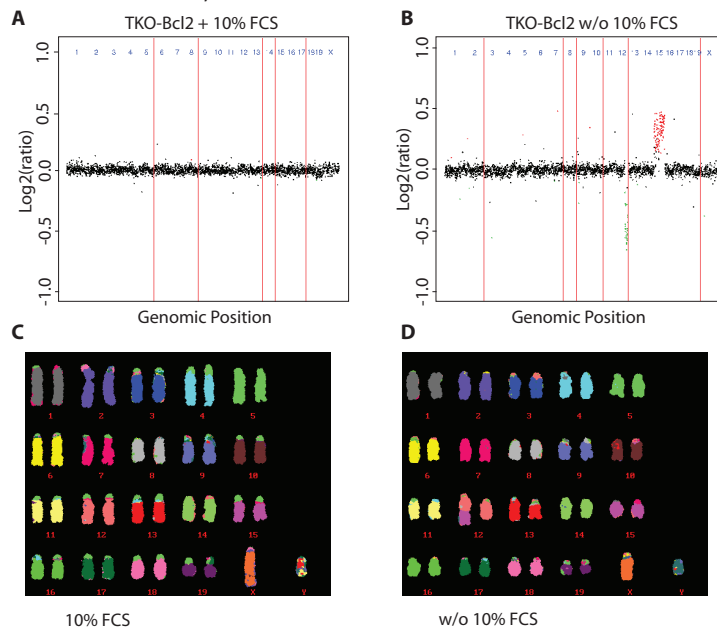


Figure 6: Single cell clones derived from serum re-stimulated TKO-Bcl2 MEFs contain CNAs

(A, B) Array-CGH profiles of clones derived from (A) TKO-Bcl2 cell cultured in 10% FCS continuously or (B) serum re-stimulated TKO-Bcl2 cell (plated 48 hours after serum re-addition). Log₂ hybridization ratios are plotted for 2,803 BAC clones, represented on the CGH microarray, at their genomic position. Red dots represent amplifications >0, and green dots represent deletions <0 (Rosetta error model; $P < 0.01$). (C, D) M-FISH analysis of cells used in panel a and b, respectively.

To investigate whether in addition to numerical alterations also structural aberrations had occurred, we applied multiplex FISH (M-FISH) to 11 TKO-Bcl2 clones derived from single cells (Table 1, clone 1-3 10% FCS and clone 1-8 w/o 10% FCS) (Jentsch et al. 2001). Strikingly, we only rarely found evidence for translocations. One clone showed an unbalanced translocation t(12;15) in 100% of the analyzed cells (Figure 6C) corresponding to the gain of chromosome 15 and partial loss of chromosome 12 detected by aCGH in this clone (Figure 6A). The M-FISH analyses generally confirmed the gains and losses detected by aCGH. However, by M-FISH we detected CNAs that were absent in the aCGH profiles, but most of the time these aberrations were present in the minority of metaphase spreads (Table 1).

Interestingly, unlike TKO-Bcl2 MEFs cultured in 10% FCS continuously (Dannenberg et al. 2000; Vormer et al. 2008), one of these genetically altered cell clones was able to form colonies in soft agar upon expression of Ras^{V12} (Figure S5). This shows that this clone had progressed towards a more transformed phenotype. Taken together, these analyses show that a temporary period of mitogen deprivation in pocket protein deficient MEFs resulted in genetically altered cell clones, mainly manifested by chromosome gains or losses that might promote tumorigenesis.

Discussion

We demonstrate here that mitogen deprivation in MEFs devoid of G1/S control (TKO-Bcl2 and *Rb*^{-/-}*p107*^{-/-} MEFs) resulted in the formation of DSBs. These DSBs are sensed by the DDR, leading to the accumulation of the cyclin dependent kinase inhibitor p21^{Cip1}. We previously showed that up-regulation of p21^{Cip1} in mitogen-deprived TKO-Bcl2 MEFs contributed to a sustained G2 arrest by inhibiting the activity of Cyclin A-CDK2 as well as Cyclin B-CDK1 complexes (Fojer et al. 2005). However, G2 arrest in mitogen-deprived TKO-Bcl2 MEFs did not solely rely on the DDR: treatment of mitogen-deprived TKO-Bcl2 MEFs with caffeine (without the addition of 10% FCS) was not sufficient to force cells into mitosis (Fojer et al. 2005), although it did reduce p21^{Cip1} levels (Figure 1D). The reason is that also the CKI p27^{Kip1} is induced upon mitogen deprivation due to reduced PI3 kinase activity (Fojer et al. 2008). Thus, p21^{Cip1} and p27^{Kip1} both contribute to G2 arrest although they are induced by different mechanisms.

Our study also revealed another type of chromosomal abnormality in mitogen-starved TKO-Bcl2 MEFs: loss of sister chromatid cohesion. Interestingly, compromised centromeric sister chromatid cohesion was also observed upon pRB depletion in RPE-1 cells and this promoted merotelic attachments (A. Manning and N. Dyson, personal communication).

Importantly, we only detected DSBs and cohesion defects in TKO-Bcl2 MEFs that were cultured in the absence but not in the presence of mitogenic stimuli. This contradicts previous findings. Normal human keratinocytes expressing HPV-16 E7 contained increased numbers of γ -H2AX foci (Duensing and Munger 2002) and Rb inactivation or expression of HPV E7 in normal human fibroblasts resulted in the formation of DSBs (Pickering and Kowalik 2006). Besides the difference in cell type, in these studies methods were used to acutely down-regulate the Rb pathway, contrary to our study where the three pocket proteins were constitutively absent. The latter may have allowed for up-regulation of compensatory pathways to counteract DSB formation in the presence of serum. Furthermore, it is uncertain whether the culture conditions were optimal in all cases. Thus, culture stress due to suboptimal culture conditions might result in DNA damage in cells deprived of Rb protein activity.

A question that remains is how culture stress, effectuated by serum deprivation, in TKO-Bcl2 MEFs resulted in the formation of DSBs and cohesion defects. Mitogen deprivation did not induce these abnormalities in WT MEFs that arrested in G1. Mitogen-deprived TKO-Bcl2 MEFs did enter S-phase, because of the absence of G1/S control, suggesting that chromosome aberrations resulted from replication stress. Previously, we have shown that the accumulation of p21^{Cip1} and p27^{Kip1} in serum-starved TKO-Bcl2 MEFs caused inhibition of Cyclin A and Cyclin B associated kinase activities (Folger et al. 2005). Cyclin A has been implicated in S-phase progression by activating the DNA polymerase δ -dependent elongation machinery (Bashir et al. 2000) and blocking Cyclin A activity inhibited progression through S-phase (Yam et al. 2002). Thus, the reduced Cyclin A associated kinase activity in serum deprived TKO-Bcl2 MEFs might cause perturbations in S-phase progression causing replication fork stalling and collapse, eventually leading to DSBs (Helleday et al. 2008). Interestingly, a DNA damage response has previously been observed upon activation of various oncogenes and has been ascribed to stalling and collapse of replication forks (Bartkova et al. 2006; Di Micco et al. 2006; Halazonetis et al. 2008). Furthermore, the establishment of sister chromatid cohesion occurs at replication forks and it has been suggested that this might also be disturbed during replication stress (Peters et al. 2008). Indirectly, defects in sister chromatid cohesion could compromise the repair of DSBs (Watrin and Peters 2006) occurring after mitogen deprivation.

We observed that serum re-stimulated TKO-Bcl2 MEFs repaired DSBs before entering mitosis since the number of cells containing γ -H2AX/Rad51 foci decreased as well as the number of 53BP1-GFP foci in single cells that were followed by time-lapse microscopy. Furthermore, cell cycle re-entry of these cells was at least partially dependent on down-regulation of the activity of the DDR since treatment with caffeine resulted in an accelerated cell cycle re-entry. Strikingly though, the majority of re-stimulated cells ended up in mitosis with several remaining chromatid breaks per cell. This may indicate that once the p27^{Kip1} protein levels were reduced by serum re-addition, the DDR, resulting in high levels of p21^{Cip1}, was not sufficiently stringent to keep DNA-damage-containing TKO-Bcl2 MEFs in G2.

The low stringency of the DDR-induced G2 arrest may be a direct consequence of loss of the Rb pathway. Indeed, several studies have shown that cells lacking Rb function had a less prominent G2 arrest in response to DNA damage due to an inability to down-regulate genes that promote G2/M progression (Hernando et al. 2004; Jackson et al. 2005; Eguchi et al. 2007). Additionally, it has been reported that a normally functioning G2/M checkpoint is not that stringent since cells with 10-20 DSBs in G2 are allowed to enter mitosis (Deckbar et al. 2007). However, the implications of a negligent G2/M checkpoint in damaged cells for genome integrity in descendent cells are not well known.

We now show that mitotic chromosomal abnormalities, like chromatid breaks and cohesion defects, can be detrimental for genomic integrity since we obtained proliferating cell clones of serum-starved and –re-stimulated TKO-Bcl2 MEFs that contained CNAs. How chromatid breaks and cohesion defects contribute to CNAs is not entirely clear. Previous work showed that uncorrected merotelic attachments can give rise to lagging chromosomes during anaphase, eventually causing mis-segregation (Cimini et al. 2001). Thus, it is likely that the defects in centromeric cohesion in serum restimulated TKO-Bcl2 MEFs resulted in the genetic alterations we observed in descendent cell clones. In line with this, it was recently demonstrated that chromatid cohesion defects resulted in chromosomal instability in human cells and were detected in a subset of human cancers (Barber et al. 2008).

Human retinoblastomas are genetically unstable (Dimaras et al. 2008), but this phenomenon has thus far not been linked to defects in DNA repair. An intriguing question is whether loss of G1/S control in combination with inappropriate growth conditions could induce genomic instability and promote oncogenic transformation in vivo.

Material and Methods

Cell culture and constructs

MEFs were isolated from chimeric embryos as described previously (Dannenberg et al. 2000), and cultured in GMEM (Invitrogen-GIBCO), supplemented with 10% fetal calf serum, 0.1mM nonessential amino acids (Invitrogen-GIBCO), 1mM sodium pyruvate (Invitrogen-GIBCO), 100µl/ml penicillin, 100µg/ml streptomycin (Invitrogen-GIBCO) and 0.1mM β-mercaptoethanol (Merck). Bcl2 expressing MEFs were generated as described previously (Foijer et al. 2005). The retroviral vector encoding 53BP1-GFP has been described (van Vugt et al.), pBABE-Ras^{V12} was kindly provided by T. Brummelkamp. TKO-Bcl2 + 53BP1-GFP MEFs and Ras^{V12} expressing cells were obtained using the same transfection/infection protocol (Foijer et al. 2005). For serum starvation experiments, cells were trypsinized and allowed to attach in the presence of serum for 4 hours. Subsequently, cells were washed with PBS and supplemented with serum free medium. For serum re-stimulation experiments, serum free medium was replaced after 7 days by complete medium. In case of caffeine or UCN-01 treatment, cells were incubated with 5mM caffeine (Sigma) or 300nM UCN-01 in serum-containing medium. UCN-01 was generously provided by Kyowa Hakko Kogyo, Co.

Immunoblots and antibodies

Cells were harvested and subsequently lysed for 30 min in ELB (150mM NaCl; 50mM Hepes pH7.5; 5mM EDTA; 0.1% NP-40) containing protease inhibitors (Complete, Roche). Protein concentrations were measured using the Bradford Assay (Biorad) or BCA protein assay kit (Pierce). For chromatin isolation cells were harvested and subsequently lysed for 30 minutes in ELB⁺ (150mM NaCl; 50mM Hepes pH7.5; 5mM EDTA; 0.5 % NP-40, 6% glycerol) containing protease inhibitors (Complete, Roche), sodiumorthovanadat, sodiumfluoride and glycerol 2-phosphate disodiumsalthydrate. After centrifugation (3 minutes at 5000rpm) the supernatant was taken as soluble fraction, the pellet was washed 3 times and used as chromatin fraction.

The used primary antibodies were rabbit polyclonal p21 (C19; Santa Cruz), mouse monoclonal p27 (BD transduction laboratory), goat CDK4 (C22; Santa Cruz), rabbit polyclonal Histone H2B (Upstate) and γ-tubulin (GTU-88; Sigma). Secondary antibodies used were HRP-conjugated Goat anti-Mouse and HRP conjugated Goat anti-Rabbit (Dako).

Immunofluorescence

For immunofluorescence stainings, cells were cultured on cover slides, washed with PBS and fixed for 5 min using 4% paraformaldehyde (Merck). Cells were permeabilized by 0.1% Triton-X100 (Sigma) in PBS for 5 min. Subsequently, cells were washed three times using staining buffer (0.15% glycine (Merck), 0.5% Bovine Serum Albumine (BSA, Sigma) in PBS) and incubated for 60 min at room temperature in staining buffer. Cells were incubated for 4h and 1h with primary and secondary antibodies, respectively. Bleaching was prevented by Vectashield (Vector Laboratories). The primary antibodies used were rabbit polyclonal Rad51 (a gift from Prof. Dr. Roland Kanaar)

and mouse monoclonal phosphorylated H2AX (Upstate) in 1:2500 and 1:100 dilutions in staining buffer, respectively. Secondary antibodies used were Alexa 488-labeled Chicken-anti-Mouse and Alexa 568-labeled Goat-anti-Rabbit antibodies (Molecular probes) and these were used in a 1:200 dilution in staining buffer. DNA was stained using To-Pro3 dye (Molecular probes).

Comet assay

Neutral comet assays were performed as described by Olive et al (Olive and Banath 2006). Briefly, 8×10^3 cells were diluted in 0.4ml PBS and added to 1.2 ml 1% low-gelling-temperature agarose (Sigma). Subsequently, the cell suspension was transferred onto pre-coated slides (Menzel-Gläser). Cell lysis was performed in neutral lysis solution (2% sarkosyl, 0.5M Na₂EDTA, 0.5 mg/ml proteinase K) pH 8.0 overnight at 37°C. Slides were washed three times with neutral rinse and electrophoresis buffer (90mM Tris, 90mM boric acid, 2mM Na₂EDTA) pH 8.5, and electrophoresis was performed in neutral rinse and electrophoresis buffer for 25 min at 20V. Nuclei were stained with 2.5µg/ml Propidium Iodide (Invitrogen) in distilled water for 20 min. Pictures of individual cells were taken with a Zeiss AxioObserver Z1 inverted microscope equipped with a cooled Hamamatsu ORCA AG Black and White CCD camera and analyzed with CASP software (<http://www.casp.of.pl>). The p-value was measured using 1-way ANOVA (nonparametric Kruskal-Wallis test).

Time-lapse microscopy

For time-lapse microscopy experiments, cells were plated on 35mm glass-bottom culture dishes (Willco-dishes). Mitogen-deprived cells were followed from 1 hour after serum re-addition until 48 hours later. For live imaging, dishes were transferred to a heated stage (37°C) on a Zeiss Axiovert 200M microscope equipped with a 0.55 numerical aperture (N.A.) condensor and a 40X Achromplan objective (N.A. = 0.60). 12 bit DIC (Digital Image Contrast) images (100msec exposure) and fluorescent images (50msec exposure) were captured every 5 min using a Photometrics Coolsnap HQ CCD camera set at gain 1.0 (Scientific, Tuscon, AZ) and appropriate filter cubes (Chroma Technology Corp.) to select specific fluorescence. Images were processed using Metamorph software (Universal Imaging, Downingtown, PA).

Flow cytometry

After fixation in ice-cold 70% ethanol, cells were stained with mouse anti-MPM2 antibody (Upstate) for 1 hour in a 1:200 dilution. The secondary antibody used was Alexa 488-labeled Chicken-anti-Mouse (Molecular Probes) in a 1:200 dilution. Subsequently, cells were counterstained with Propidium Iodide diluted in PBS containing RNase. Finally, the percentage of mitotic cells (MPM2 positivity) and the cell cycle distribution (Propidium Iodide) of the cells were determined by flow cytometry, using "Cell Quest" software (BD Bioscience).

Chromosome spreads

For chromosome spreads, mitogen-deprived MEFs were serum re-stimulated for 21 hours and treated with 0.2µg/ml colcemid (Sigma) during the last 45 min to trap cells in mitosis or treated with only 50nM Calyculin A (Invitrogen) for 30 minutes. Cells were forced to swell using 75mM KCl for 10 min and subsequently fixed by a 3:1 mixture of methanol and acetic acid. Prior to light microscopy, cells were spread on microscope slides. Per condition 50 spreads were analyzed for chromosome breakage events and loss of centromeric cohesion. We scored the number of

chromatid breaks as well as chromatid interchanges as described in Joenje et al (Joenje et al. 1981). Dependent on its complexity, a chromatid interchange was counted as one or two breaks. The numbers of chromatid breaks derived from chromatid interchanges per total number of break events per culture were as follows: WT +10% FCS: 2/18, TKO-Bcl2 +10% FCS: 0/1, WT w/o 10% FCS: 4/8, TKO-Bcl2 w/o 10% FCS: 14/172. We did not find chromosome break events.

Genomic DNA isolation, fragmentation, labeling and BAC array hybridization

Genomic DNA from test and control TKO MEFs was extracted and purified with the DNeasy blood and tissue kit (Qiagen). Subsequently, DNA was fragmented using the Bioruptor (Diagenode). Fragment sizes were checked on a 1% agarose gel (100 – 600bp). Test and reference DNA were labeled with the Kreatech ULS array CGH labeling kit (Kreatech). Test DNA was derived from single cell clones of serum re-stimulated TKO-Bcl2 MEFs (plated either 48 hours after serum re-addition (whole population) or 21 hours after serum re-addition (mitotic cells only) and single cell clones of TKO-Bcl2 MEFs cultured in the presence of 10% FCS continuously. As reference DNA we used genomic DNA isolated from TKO-Bcl2 MEFs cultured in the presence of 10% FCS continuously. The fluorescently labeled DNA was hybridized on a 3K mouse BAC microarray as described previously (Chung et al. 2004). The Rosetta error model was used to calculate weighted averages and statistical confidence levels. All values with *P* values <0.01 were considered to represent significant CNAs.

M-FISH

Single cell clones were cultured and treated with 0.02µg/ml colcemid (Sigma) for 2 hours to obtain metaphase-arrested cells. Cells were subjected to an osmotic shock (75mM KCl) for 10 min and fixed in 3:1 methanol:acetic acid. Prior to hybridization cells were dropped on microscope slides, aged overnight and treated with 0.01% pepsin (Sigma) for 5 minutes. Slides were baked at 65°C for 1h before denaturation at 63°C in 70% formamide/2xSSC and then dehydrated through an ethanol series (70, 90 and 100%). Individual mouse paints were prepared using flow sorted mouse chromosomes as described previously (Jentsch et al. 2001). The 'mouse paint mix' was prepared using whole chromosome-specific paints labeled with a different combination of 4 fluorochromes (Cy5, Texas Red, Cy3 and FITC) and one hapten (Biotin). Each chromosome in the mix was labeled with a unique combination of 3 or less fluorochromes except for chromosome Y which was labeled with all 5. Mouse paint was denatured at 65°C for 10 min and 7µl of paint was applied to each slide. Slides were incubated at 37°C for 48 hours, washed in 50% formamide/2xSSC at 43°C and then incubated with one layer of Streptavidin Dylight 680 conjugate (Thermo Fisher Scientific) for biotin. Slides were counterstained with 10µl of 4,6, diamidino-2-phenylindole (DAPI) counter stain in antifade. Images of metaphase spreads were captured using a Leica 5000DM epifluorescent microscope equipped with narrow bandpass filter sets for DAPI, FITC, Cy3, Texas Red, Cy5, and Cy5.5 and a cooled charge coupled device (CCD) camera. For each metaphase spread, six images were captured using filter combinations specific for each of the five fluorochromes and DAPI. A minimum of 10 metaphases were captured from each cell line and analyzed using Leica CW 4000 CytoFISH software.

Soft agar assay

Soft agar assays were performed as described previously (Vormer et al. 2008). Briefly, 6x10⁴ MEFs were suspended in 0,35% soft agar solution and plated on one well of a six-well plate and

incubated at 37°C for three weeks. Pictures were taken using a non-phase-contrast lens (x2.5 magnification) and assembled using Axiovision 4.5.

Acknowledgements

We thank R. Kanaar for rabbit polyclonal Rad51 antibody, Kyowa Hakko Kogyo Company for UCN-01 and B. Fu for the M-FISH reagents. We thank L. Oomen and L. Brocks for help with the microscopical visualization of the comets, W. van Zon for help with time-lapse microscopy and W. Brugman for help with aCGH. We are grateful to N. Carter, T. Vormer, S. Bakker and M. Aarts for fruitful discussions and critically reading the manuscript. This work was supported by the Dutch Cancer Society (NKI 2007–3790) and the Wellcome Trust (grant number WT077008).

References

- Amato, A., Lentini, L., Schillaci, T., Iovino, F., and Di Leonardo, A. 2009. RNAi mediated acute depletion of retinoblastoma protein (pRb) promotes aneuploidy in human primary cells via micronuclei formation. *BMC Cell Biol* **10**: 79.
- Barber, T.D., McManus, K., Yuen, K.W., Reis, M., Parmigiani, G., Shen, D., Barrett, I., Nouhi, Y., Spencer, F., Markowitz, S. et al. 2008. Chromatid cohesion defects may underlie chromosome instability in human colorectal cancers. *Proc Natl Acad Sci U S A* **105**(9): 3443-3448.
- Bartkova, J., Rezaei, N., Lontos, M., Karakaidos, P., Kleitas, D., Issaeva, N., Vassiliou, L.V., Kolettas, E., Niforou, K., Zoumpourlis, V.C. et al. 2006. Oncogene-induced senescence is part of the tumorigenesis barrier imposed by DNA damage checkpoints. *Nature* **444**(7119): 633-637.
- Bashir, T., Horlein, R., Rommelaere, J., and Willwand, K. 2000. Cyclin A activates the DNA polymerase delta -dependent elongation machinery in vitro: A parvovirus DNA replication model. *Proc Natl Acad Sci U S A* **97**(10): 5522-5527.
- Bosco, E.E., Mayhew, C.N., Hennigan, R.F., Sage, J., Jacks, T., and Knudsen, E.S. 2004. RB signaling prevents replication-dependent DNA double-strand breaks following genotoxic insult. *Nucleic Acids Res* **32**(1): 25-34.
- Branzei, D. and Foiani, M. 2008. Regulation of DNA repair throughout the cell cycle. *Nat Rev Mol Cell Biol* **9**(4): 297-308.
- Burkhardt, D.L. and Sage, J. 2008. Cellular mechanisms of tumour suppression by the retinoblastoma gene. *Nat Rev Cancer* **8**(9): 671-682.
- Chung, Y.J., Jonkers, J., Kitson, H., Fiegler, H., Humphray, S., Scott, C., Hunt, S., Yu, Y., Nishijima, I., Velds, A. et al. 2004. A whole-genome mouse BAC microarray with 1-Mb resolution for analysis of DNA copy number changes by array comparative genomic hybridization. *Genome Res* **14**(1): 188-196.
- Cimini, D., Howell, B., Maddox, P., Khodjakov, A., Degraffi, F., and Salmon, E.D. 2001. Merotelic kinetochore orientation is a major mechanism of aneuploidy in mitotic mammalian tissue cells. *J Cell Biol* **153**(3): 517-527.
- Corson, T.W. and Gallie, B.L. 2007. One hit, two hits, three hits, more? Genomic changes in the development of retinoblastoma. *Genes Chromosomes Cancer* **46**(7): 617-634.
- Dannenberg, J.H., Schuijff, L., Dekker, M., van der Valk, M., and te Riele, H. 2004. Tissue-specific tumor suppressor activity of retinoblastoma gene homologs p107 and p130. *Genes Dev* **18**(23): 2952-2962.
- Dannenberg, J.H., van Rossum, A., Schuijff, L., and te Riele, H. 2000. Ablation of the retinoblastoma gene family deregulates G(1) control causing immortalization and increased cell turnover under growth-restricting conditions. *Genes Dev* **14**(23): 3051-3064.
- Deckbar, D., Birraux, J., Krempler, A., Tchouandong, L., Beucher, A., Walker, S., Stiff, T., Jeggo, P., and Lobrich, M. 2007. Chromosome breakage after G2 checkpoint release. *J Cell Biol* **176**(6): 749-755.
- Di Micco, R., Fumagalli, M., Cicalese, A., Piccinin, S., Gasparini, P., Luise, C., Schurra, C., Garre, M., Nuciforo, P.G., Bensimon, A. et al. 2006. Oncogene-induced senescence is a DNA damage response triggered by DNA hyper-replication. *Nature* **444**(7119): 638-642.
- Dimaras, H., Khetan, V., Halliday, W., Orlic, M., Prigoda, N.L., Piovesan, B., Marrano, P., Corson, T.W., Eagle, R.C., Jr., Squire, J.A. et al. 2008. Loss of RB1 induces non-proliferative retinoma: increasing genomic instability correlates with progression to retinoblastoma. *Hum Mol Genet* **17**(10): 1363-1372.
- Doorbar, J. 2006. Molecular biology of human papillomavirus infection and cervical cancer. *Clin Sci (Lond)* **110**(5): 525-541.
- Duensing, S. and Munger, K. 2002. The human papillomavirus type 16 E6 and E7 oncoproteins independently induce numerical and structural chromosome instability. *Cancer Res* **62**(23): 7075-7082.
- Eguchi, T., Takaki, T., Itadani, H., and Kotani, H. 2007. RB silencing compromises the DNA damage-

- p induced G2/M checkpoint and causes deregulated expression of the ECT2 oncogene.
- Onco-
gene*
- 26**
- (4): 509-520.
- Foijer, F., Simonis, M., van Vliet, M., Wessels, L., Kerkhoven, R., Sorger, P.K., and Te Riele, H. 2008. On-
cogenic pathways impinging on the G2-restriction point. *Oncogene* **27**(8): 1142-1154.
- Foijer, F., Wolthuis, R.M., Doodeman, V., Medema, R.H., and te Riele, H. 2005. Mitogen requirement
for cell cycle progression in the absence of pocket protein activity. *Cancer Cell* **8**(6): 455-466.
- Gonzalo, S., Garcia-Cao, M., Fraga, M.F., Schotta, G., Peters, A.H., Cotter, S.E., Eguia, R., Dean, D.C.,
Esteller, M., Jenuwein, T. et al. 2005. Role of the RB1 family in stabilizing histone methylation
at constitutive heterochromatin. *Nat Cell Biol* **7**(4): 420-428.
- Gotoh, E. 2009. Drug-induced premature chromosome condensation (PCC) protocols: cytogenetic ap-
proaches in mitotic chromosome and interphase chromatin. *Methods Mol Biol* **523**: 83-92.
- Graves, P.R., Yu, L., Schwarz, J.K., Gales, J., Sausville, E.A., O'Connor, P.M., and Piwnica-Worms, H. 2000.
The Chk1 protein kinase and the Cdc25C regulatory pathways are targets of the anticancer
agent UCN-01. *J Biol Chem* **275**(8): 5600-5605.
- Halazonetis, T.D., Gorgoulis, V.G., and Bartek, J. 2008. An oncogene-induced DNA damage model for
cancer development. *Science* **319**(5868): 1352-1355.
- Harper, J.W. and Elledge, S.J. 2007. The DNA damage response: ten years after. *Mol Cell* **28**(5): 739-745.
- Helleday, T., Petermann, E., Lundin, C., Hodgson, B., and Sharma, R.A. 2008. DNA repair pathways as
targets for cancer therapy. *Nat Rev Cancer* **8**(3): 193-204.
- Hernando, E., Nahle, Z., Juan, G., Diaz-Rodriguez, E., Alaminos, M., Hemann, M., Michel, L., Mittal, V.,
Gerald, W., Benezra, R. et al. 2004. Rb inactivation promotes genomic instability by uncou-
pling cell cycle progression from mitotic control. *Nature* **430**(7001): 797-802.
- Iovino, F., Lentini, L., Amato, A., and Di Leonardo, A. 2006. RB acute loss induces centrosome amplifica-
tion and aneuploidy in murine primary fibroblasts. *Mol Cancer* **5**: 38.
- Jackson, M.W., Agarwal, M.K., Yang, J., Bruss, P., Uchiumi, T., Agarwal, M.L., Stark, G.R., and Taylor,
W.R. 2005. p130/p107/p105Rb-dependent transcriptional repression during DNA-damage-
induced cell-cycle exit at G2. *J Cell Sci* **118**(Pt 9): 1821-1832.
- Jentsch, I., Adler, I.D., Carter, N.P., and Speicher, M.R. 2001. Karyotyping mouse chromosomes by mul-
tiplex-FISH (M-FISH). *Chromosome Res* **9**(3): 211-214.
- Joenje, H., Arwert, F., Eriksson, A.W., de Koning, H., and Oostra, A.B. 1981. Oxygen-dependence of
chromosomal aberrations in Fanconi's anaemia. *Nature* **290**(5802): 142-143.
- Knudsen, K.E., Booth, D., Naderi, S., Sever-Chroneos, Z., Fribourg, A.F., Hunton, I.C., Feramisco, J.R.,
Wang, J.Y., and Knudsen, E.S. 2000. RB-dependent S-phase response to DNA damage. *Mol
Cell Biol* **20**(20): 7751-7763.
- Malumbres, M. and Barbacid, M. 2001. To cycle or not to cycle: a critical decision in cancer. *Nat Rev
Cancer* **1**(3): 222-231.
- Marx, J. 2002. Debate surges over the origins of genomic defects in cancer. *Science* **297**(5581): 544-
546.
- Mayhew, C.N., Bosco, E.E., Fox, S.R., Okaya, T., Tarapore, P., Schwemberger, S.J., Babcock, G.F., Lentsch,
A.B., Fukasawa, K., and Knudsen, E.S. 2005. Liver-specific pRB loss results in ectopic cell cycle
entry and aberrant ploidy. *Cancer Res* **65**(11): 4568-4577.
- Medema, R.H., Kops, G.J., Bos, J.L., and Burgering, B.M. 2000. AFX-like Forkhead transcription factors
mediate cell-cycle regulation by Ras and PKB through p27kip1. *Nature* **404**(6779): 782-787.
- Olive, P.L. and Banath, J.P. 2006. The comet assay: a method to measure DNA damage in individual
cells. *Nat Protoc* **1**(1): 23-29.
- Paull, T.T., Rogakou, E.P., Yamazaki, V., Kirchgessner, C.U., Gellert, M., and Bonner, W.M. 2000. A critical
role for histone H2AX in recruitment of repair factors to nuclear foci after DNA damage. *Curr
Biol* **10**(15): 886-895.
- Perez-Ordonez, B., Beauchemin, M., and Jordan, R.C. 2006. Molecular biology of squamous cell carci-
noma of the head and neck. *J Clin Pathol* **59**(5): 445-453.
- Peters, J.M., Tedeschi, A., and Schmitz, J. 2008. The cohesin complex and its roles in chromosome biol-
ogy. *Genes Dev* **22**(22): 3089-3114.

- Pickering, M.T. and Kowalik, T.F. 2006. Rb inactivation leads to E2F1-mediated DNA double-strand break accumulation. *Oncogene* **25**(5): 746-755.
- Sage, J., Mulligan, G.J., Attardi, L.D., Miller, A., Chen, S., Williams, B., Theodorou, E., and Jacks, T. 2000. Targeted disruption of the three Rb-related genes leads to loss of G(1) control and immortalization. *Genes Dev* **14**(23): 3037-3050.
- Sarkaria, J.N., Busby, E.C., Tibbetts, R.S., Roos, P., Taya, Y., Karnitz, L.M., and Abraham, R.T. 1999. Inhibition of ATM and ATR kinase activities by the radiosensitizing agent, caffeine. *Cancer Res* **59**(17): 4375-4382.
- Schultz, L.B., Chehab, N.H., Malikzay, A., and Halazonetis, T.D. 2000. p53 binding protein 1 (53BP1) is an early participant in the cellular response to DNA double-strand breaks. *J Cell Biol* **151**(7): 1381-1390.
- Srinivasan, S.V., Mayhew, C.N., Schwemberger, S., Zagorski, W., and Knudsen, E.S. 2007. RB loss promotes aberrant ploidy by deregulating levels and activity of DNA replication factors. *J Biol Chem* **282**(33): 23867-23877.
- van Vugt, M.A., Gardino, A.K., Linding, R., Ostheimer, G.J., Reinhardt, H.C., Ong, S.E., Tan, C.S., Miao, H., Keezer, S.M., Li, J. et al. A mitotic phosphorylation feedback network connects Cdk1, Plk1, 53BP1, and Chk2 to inactivate the G(2)/M DNA damage checkpoint. *PLoS Biol* **8**(1): e1000287.
- Vormer, T.L., Foijer, F., Wielders, C.L., and te Riele, H. 2008. Anchorage-independent growth of pocket protein-deficient murine fibroblasts requires bypass of G2 arrest and can be accomplished by expression of TBX2. *Mol Cell Biol* **28**(24): 7263-7273.
- Watrin, E. and Peters, J.M. 2006. Cohesin and DNA damage repair. *Exp Cell Res* **312**(14): 2687-2693.
- Yam, C.H., Fung, T.K., and Poon, R.Y. 2002. Cyclin A in cell cycle control and cancer. *Cell Mol Life Sci* **59**(8): 1317-1326.
- Yamamoto, A., Taki, T., Yagi, H., Habu, T., Yoshida, K., Yoshimura, Y., Yamamoto, K., Matsushiro, A., Nishimune, Y., and Morita, T. 1996. Cell cycle-dependent expression of the mouse Rad51 gene in proliferating cells. *Mol Gen Genet* **251**(1): 1-12.
- Zheng, L., Flesken-Nikitin, A., Chen, P.L., and Lee, W.H. 2002. Deficiency of Retinoblastoma gene in mouse embryonic stem cells leads to genetic instability. *Cancer Res* **62**(9): 2498-2502.

Supplementary Information

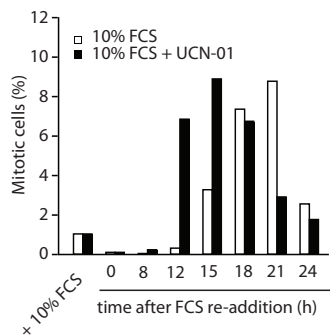
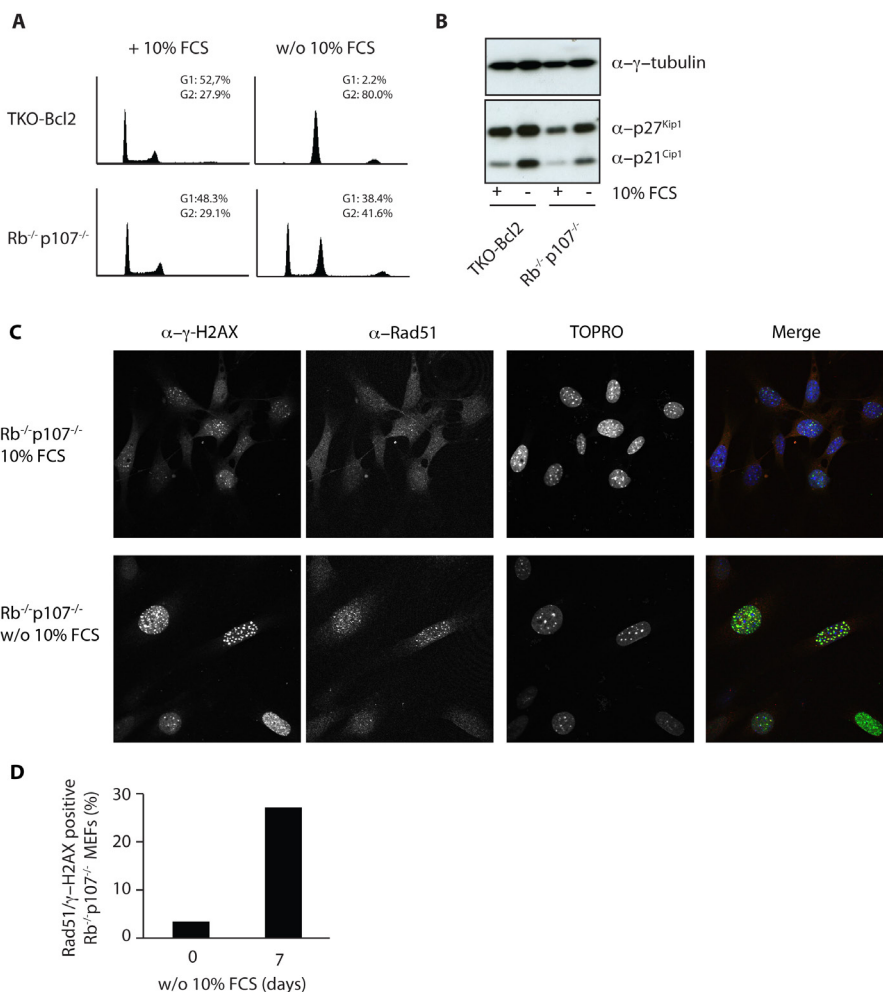


Figure S1: Inhibition of the DDR results in accelerated cell cycle re-entry of G2-arrested TKO-Bcl2 MEFs after serum re-addition

Percentage of mitotic cells in TKO-Bcl2 MEFs at different timepoints after serum re-addition either in the presence (black bars) or in the absence (white bars) of UCN-01.



< Figure S2: Serum deprived (7 days) *Rb*^{-/-} *p107*^{-/-} MEFs partially arrest in G2 and show signs of DNA damage

(A) Cell cycle distribution in TKO-Bcl2 and *Rb*^{-/-} *p107*^{-/-} MEFs cultured in the presence (+) or absence (w/o) of 10% FCS. (B) p27^{Kip1} and p21^{Cip1} protein levels in TKO-Bcl2 and *Rb*^{-/-} *p107*^{-/-} MEFs cultured in the presence or absence of 10% FCS. Anti γ -tubulin was used as loading control. (C) Immunofluorescent images of *Rb*^{-/-} *p107*^{-/-} MEFs cultured in the presence or absence of 10% FCS to detect γ -H2AX and Rad51 foci. DNA was labeled with TOPRO-3. In the merge picture DNA is blue, γ -H2AX is green, Rad51 is red and colocalization of γ -H2AX and Rad51 is seen as yellow foci. (D) Quantification of γ -H2AX/Rad51 focus formation in *Rb*^{-/-} *p107*^{-/-} MEFs cultured in the presence or absence of 10%FCS. Cells were considered positive when they contained five or more superimposed γ -H2AX and Rad51 foci. At least 100 cells were counted for each condition.

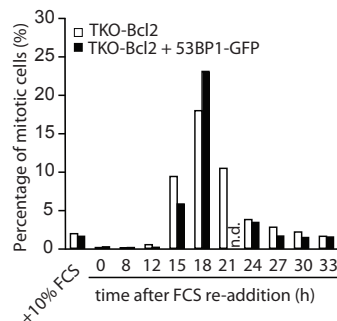


Figure S3: Expression of 53BP1-GFP does not interfere with mitotic entry of G2-arrested TKO-Bcl2 MEFs after serum re-addition

Percentage of mitotic cells in either mitogen-deprived TKO-Bcl2 MEFs (white bars) or mitogen-deprived TKO-Bcl2 MEFs transduced with 53BP1-GFP (black bars) at different time points after serum re-addition. (n.d.) not determined.

2

GENOMIC INSTABILITY IN Rb-DEFICIENT CELLS